Tuning adhesion failure strength for tissue-specific applications

Citation: Artzi, Natalie, Adam Zeiger, Fiete Boehning, Adriana bon Ramos, Krystyn Van Vliet, and Elazer R. Edelman. "Tuning Adhesion Failure Strength for Tissue-Specific Applications." Acta Biomaterialia 7, no. 1 (January 2011): 67–74.

As Published: http://dx.doi.org/10.1016/j.actbio.2010.07.008

Publisher: Elsevier

Persistent URL: http://hdl.handle.net/1721.1/99200

Version: Author's final manuscript: final author's manuscript post peer review, without publisher's formatting or copy editing

Published in final edited form as:
Acta Biomater. 2011 January ; 7(1): 67–74. doi:10.1016/j.actbio.2010.07.008.

Tuning Adhesion Failure Strength For Tissue-Specific Applications

Natalie Artzi[a,b], **Adam Zeiger**[c], **Fiete Boehning**[a], **Adriana bon Ramos**[a,d], **Krystyn Van Vliet**[c], and **Elazer R. Edelman**[a,e]

[a]Harvard–MIT Division of Health Sciences and Technology, Massachusetts Institute of Technology, Cambridge, Massachusetts 02139

[b]Anasthesiology Division, Brigham and Women's Hospital, Harvard Medical School, Boston, Massachusetts 02115

[c]Materials Science and Engineering, Massachusetts Institute of Technology, Cambridge, Massachusetts 02139

[d]Department of Chemistry, Institut Quiimic de Sarriá, Universitat Ramon Llull, Barcelona, Spain 08017

[e]Cardiovascular Division, Department of Medicine, Brigham and Women's Hospital, Harvard Medical School, Boston, Massachusetts 02115

Abstract

Soft tissue adhesives are employed to repair and seal multiple organs, which range in both tissue surface chemistry and mechanical challenges during organ function. This complexity motivates the development of tunable adhesive materials with high resistance to uniaxial or multiaxial loads dictated by a specific organ environment. Co-polymeric hydrogels comprising aminated star polyethylene glycol and dextran aldehyde (PEG:dextran) are materials exhibiting physicochemical properties that can be modified to achieve this organ- and tissue-specific adhesion performance. Here we report that resistance to failure under specific loading conditions, as well as tissue response at the adhesive material-tissue interface, can be modulated through regulation of number and density of adhesive aldehyde groups. We find that atomic force microscopy (AFM) can characterize material aldehyde density available for tissue interaction, and in this way enable rapid, informed material choice. Further, the correlation between AFM quantification of nanoscale unbinding forces with macroscale measurements of adhesion strength by uniaxial tension or multiaxial burst pressure allows for the design of materials with specific cohesion and adhesion strengths. However, failure strength alone does not predict optimal *in vivo* reactivity. Thus, we demonstrate that the development of adhesive materials is enabled significantly when experiments are integrated along lengthscales to consider organ chemistry and mechanical loading states concurrently with adhesive material properties and tissue response.

Corresponding author: Natalie Artzi, Ph.D., Harvard-MIT Division for Health Sciences and Technology, Massachusetts Institute of Technology, E25-449, 77 Massachusetts Ave., Cambridge, MA 02139 (USA), nartzi@mit.edu, tel: (617)253-8146, fax:(617)253-2514.

Keywords

Adhesion; AFM; Biocompatibility; Mechanical properties; Tissue adhesive

Introduction

Adhesive materials expand significantly the resources available for wound repair and surgical interventions.[1-3] Synthetic adhesives can enhance support and augmentation of soft-tissue organs such as the heart and intestine, or hard-tissues such as bone and teeth.[4-6] However, this wide array of target tissue applications provides a unique challenge, requiring adhesive materials that differ greatly in their physicochemical properties to meet the varying demands of a wide range of tissue compositions and mechanical loading conditions. Commercially available adhesive sealants such as fibrin glue and cyanoacrylates often require a choice between degree of adhesion and biocompatibility.[7-9] Modification of the adhesive material composition or macromolecular chain architecture can modulate adhesion without pushing this balance towards toxicity. For example, the addition of biomimetic functional groups, such as L-3,4-dihydroxylphenylalanine (DOPA), can enhance adhesion of materials to surfaces and tissues [10] through fully reversible, noncovalent interactions.[11] Alternatively, nanopatterned surfaces increase contact surface area between the adhesive [12] and tissue. However, neither this general DOPA addition nor surface topographical roughening is specific to the morphology of the target tissue or the mechanical requirements of the target organ.

This issue of tissue responsiveness takes on increased importance, given the recently demonstrated capacity to modulate the extent of tissue interaction with synthetic adhesive polymers in a tissue-specific manner.[13] For example, we have shown that PEG:dextran aldehyde copolymer materials bind differentially to lung, liver, heart or small intestine; this tissue-specific contrast is consistent with the concept that each tissue presents a different landscape of surface amines for interaction with adhesive material aldehydes. Thus, in such a material system, adhesion and biocompatibility are optimized through modulation of amine:aldehyde interactions.[13] As the field moves to design and application of such materials with tissue-specific modulated adhesion, knowledge of surface properties of both the target tissue and the adhesive becomes paramount. Further, the loading state of the adhesive in the tissue or organ application of interest must be considered, to distinguish between potential adhesive and cohesive failure modes of the tissue-adhesive material seal.

The PEG:dextran family of materials provides a model system for examining chemically directed adhesion. [13,14] There exist at least six different parameters that can be varied to create materials with the full spectrum of adhesion, including solid content and molecular weight of the two components; degree of aldehyde oxidation; and number of arms in the stellate PEG .[15] A crosslinked network of PEG:dextran is formed via binding between aldehydes and amines. Those aldehydes that are still free remain reactive, such that adhesive bonds can form between this network and opposing amines of adjacent tissues. However, an excess of aldehydes can give rise to a toxic tissue response. Identification of design parameters that maximize adhesion while minimizing adverse tissue response requires efficient materials characterization at complex interfaces.

In this study of PEG:dextran adhesives of variable composition, we demonstrate and correlate experimental approaches that can be used to quantify tissue-adhesive interactions relevant to mechanical challenges of soft-tissue adhesives *in vivo*. Atomic force microscopy (AFM)-mediated force spectroscopy can characterize the aldehyde density of such synthetic adhesive materials available for tissue interaction, and in this way enable rapid, informed material choice. Here, cantilevered AFM probes were functionalized with amines to mimic tissue

surfaces, and used to quantify interaction potential with a compositionally varied series of aldehyde-presenting adhesive gels. Adhesion strength between these characterized gels and tissue comprising the small intestine was measured *ex vivo* at the macroscale. The macroscale failure loads and pressures correlated with the unbinding force measured via AFM force spectroscopy when aldehyde groups number varied (compositions A-C), but did not correlate when aldehyde density was altered (compositions A vs. D). As anticipated, maximal adhesion strength *ex vivo* does not necessarily correlate with optimized *in vivo* function: those adhesive gels exhibiting excess aldehyde groups resulted in increased inflammation of the small intestine *in vivo*. Thus, the development of adhesive materials can advance most rapidly when experiments are integrated to consider the chemistry and mechanical loading state of the target organ concurrently with adhesive properties and tissue response.

Materials and Methods

Synthesis and formation of PEG:dextran

Star PEG amine, dextran aldehydes and PEG:dextran networks were fabricated as described previously. [13,15] Briefly, eight-arm 10 kDa star PEG polymer with amine terminal groups was dissolved in water to 10-50 wt% solutions. Linear dextran (10 kDa) was oxidized with sodium periodate to create dextran aldehyde (50% oxidation of glucose rings, 2 aldehyde groups per oxidized glucose ring), which was also prepared as an aqueous solution (8.75–23 wt%). The two homogeneous polymer solutions were loaded into a dual-chamber syringe equipped with a 12-step mixing tip. The PEG:dextran network formation occurred within seconds to minutes, following the controlled mixing of PEG amine and dextran aldehyde via a Schiff's base reaction between the constituent reactive groups (aldehydes and amines).

Selection and designation of PEG:dextran variants

Solid content, molecular weight and reactive group content of both PEG amine and dextran aldehyde polymers can be altered to create variable crosslinked networks and material properties. As the ratio of aldehyde to amine reactive group concentrations, designated as $CHO:NH_2$, is held constant, the formulations under study are meaningfully differentiated by the total number of aldehydes. To evaluate the importance of aldehyde density on the resulting material performance, dextran oxidation level (hereafter, termed % oxidation) was altered while keeping the total number of aldehydes constant (see Table1).

Atomic Force Microscopy (AFM)- spectroscopy of adhesive unbinding forces

To compare the unbinding force between PEG:dextran aldehyde-presenting materials and opposing amine-presenting surfaces, AFM-enabled force spectroscopy was conducted. Silicon cantilevers terminating in colloidal silica spheres of nominal radius $R = 1$ μm (Nanosensors, Neuchatel, Switzerland) were cleaned via ozone treatment. Probes were then functionalized with amine groups via chemical vapor deposition using evaporation of 3-(aminoproyl) triethoxysilane (APTES) and N,N-diisopropylethylamine within a dessicator for 2 hrs.

Calibration of inverse optical lever sensitivity in terms of the photodiode voltage (nm/V) and cantilever spring constant k (nominally 0.1 N/m) were conducted as previously described. [16] Samples were immersed and fully hydrated in phosphate buffered saline upon polymerization, and acquired probe deflection-piezoactuator displacement responses during approach and retraction from the adhesive material surfaces were converted offline (Scanning Probe Imaging Processor, Image Metrology) to force-distance responses. Maximum loads and contact areas were 5 nN and 2.4 μm^2, respectively, in order to sample multimolecular rather than single-molecular interactions. Contact areas were calculated from the measured depth of indentation and the manufacturer-measured radius of these AFM spherical probes (1 μm). Unbinding force (F_R) is defined herein as the force required to separate the amine-

functionalized probe from the surface of the adhesive, and serves as an indicator of the number of free aldehyde groups [17,18] available to bind. The approach and separation velocities for all samples and replicate measurements was 6 μm/s, resulting in unloading rates that did not differ among samples significantly (ANOVA, $p < 0.05$). At least 30 replicate measurements were acquired per hydrated adhesive sample.

Macroscale interfacial adhesion strength and burst pressure measurements

Adult Sprague-Dawley rats (250-300g, Charles River Laboratories, MA) were sacrificed via carbon dioxide asphyxiation under university IACUC protocol and federal guidelines for animal care. Following sacrifice, the duodenum (i.e., first section of the small intestine) was excised and immersed in 10 mL phosphate buffered saline (PBS, 150 mM NaCl) at room temperature for macroscale characterization of adhesion strength and burst pressure. Selection of this animal model enable the number of *in vitro* macroscale experiments required to establish statistical significance in potential differences in tissue-adhesion performance among the PEG:dextran materials.

To quantify macroscale adhesion strength of explanted tissue, each PEG:dextran adhesive gel was applied between two uniformly sized rat duodenal biopsies (8 mm diameter). After allowing for polymerization at the tissue interfaces (5 min), monotonic uniaxial tensile testing (Bose® Biodynamic Test Instrument, Minnetonka, MN) was employed at a constant rate (0.05 mm/sec) and the load response was continuously recorded (200 measurements/sec) to the point of macroscopic failure.

To quantify adhesive gel performance under mechanical loading related to the small intestine function in vivo, longitudinal duodenal segments were cut and inserted into a mechanical testing apparatus configured for luminal perfusion (Bose® Biodynamic Test Instrument, Minnetonka, MN). The basis of this macroscopic test is to apply internal pressure to hollow organs or tissue sections, identifying failure in terms of the fluid pressure at which catastrophic mechanical failure occurs (i.e., burst pressure). A wound was introduced by puncturing the intestinal wall with an 18-gauge needle. Wounds were then repaired with 200 μl application of PEG:dextran adhesive. After 5 min curing time, pulsatile loads were applied through the perfusion with phosphate buffered saline (PBS).The burst pressure of repaired intestinal wounds was measured through gradual increase of lumen pressure. A slow development of pressure was achieved through restriction of flow distal to the sample lumen and monitored at the inlet of the intestine. The burst pressure was easily detected, as failure of the repair site resulted in immediate loss of pressure and visible PBS leakage. The maximum luminal pressure prior to interface failure was recorded as the wound burst pressure.

Adhesive interface morphology

To investigate the morphology of the interface between these adhesives and the duodenal tissue, the surface of biopsied longitudinal rat duodenal tissues was covered with fluorescently labeled PEG:dextran (fluorescein conjugated PEG:dextran) and the material was allowed to cure for 10 min. Tissue samples were then cryosectioned (20 μm sections) and cells' nuclei stained with DAPI (Vector Laboratories).

Morphology of the tissue:material interface was quantified as intensity of fluorescein at the interface using image analysis (Leica Microsystems, MetaMorph®).

In vivo biocompatibility

To investigate the effect of aldehyde content on tissue:material interaction and biocompatibility, two material formulations containing 8.75 or 15wt% dextran aldehyde (D10-50-8,75 P8-10-25 or D10-50-14 P8-10-40) were applied to wounded small intestinal

tissues of New Zealand rabbits, and tissue response/repair was evaluated. This animal model has been demonstrated to be highly sensitive to tissue-material interactions of the duodenum, representing a more significant in vivo challenge than rat duodenum characterized *in vitro*. All experimental protocols were approved by the MIT Animal Care and Use Committee and were in compliance with NIH guidelines for animal use. Longitudinal cuts of 1 cm length were generated and 5-0 PDS II sutures were applied to close the wound. PEG:dextran sealants were applied on top of the sutures and allowed to cure for 5 min. Small intestinal tissues were harvested after 15 days, sectioned using cryotome to create 20 μm thick sections. Hematoxylin and eosin staining were performed using standard methods. Histopathological scoring via light microscopy was used to determine degree of inflammation, necrosis, hemorrhage, re-epithelialization, fibrosis and/or reactive fibrovascular proliferation that reflects the extent of the host response/repair process to the treatment with bioadhesive. Scores of 0-3 were assigned to samples to indicate no, mild, notable or marked feature present at the interface, respectively.

Statistical analysis

All macroscale data are presented as means ± standard deviation among samples, except for AFM measurements that are presented as means ± standard error among replicate measurements on a single sample. Statistical analyses were performed using one-way ANOVA with Tukey analysis post tests. A p-value < 0.05 is considered statistically significant.

Results

Four PEG:dextran adhesive formulations were studied (Table 1). Compositions A through C consider variation in the relative number of free aldehyde groups. Compositions A and D provide comparison of aldehyde group density (i.e., number of aldehyde groups per chain, via the extent of dextran oxidation), while attempting to maintain the overall number of free aldehyde groups per unit volume constant. Below we outline results characterizing the material, the *in vitro* tissue adhesion strength and failure, and the *in vivo* biocompatibility as a function of these compositional variables.

A. AFM force spectroscopic analysis of unbinding force

We employed AFM-enabled force spectroscopy to compare unbinding forces among PEG:dextran material formulations, as a molecular-scale screening tool for adhesion of these polymer adhesives to the amine-rich surfaces of tissues *in vivo.* AFM-cantilevered probes functionalized with amine groups (Fig. 1a) were used to determine the unbinding force F_R between tissue and PEG:dextran adhesive formulations. The micrometer-scale probe amines interact exclusively with free aldehydes at the polymeric gel surfaces, and the unbinding force required to separate the amine-functionalized probe is therefore a measure of aldehyde binding potential. Note that this is not intended to be a single-molecule level analysis of molecular unbinding, but rather provides a more controlled interface than tissues to explore the strength of multiple interactions at the micrometer-scale. Variation in the relative number of free aldehyde groups (compositions A-C) significantly affected F_R (ranging from 0.31±0.09 nN to 1.00±0.25 nN, with ANOVA $p < 0.001$), demonstrating the direct modulation of aldehyde-mediated adhesion efficiency via polymer design (Figure 1b).

The effect of aldehyde group density imparted by changing dextran aldehyde oxidation from 20 to 50% (compositions A and D) is less intuitive. Here, composition D presents a lower aldehyde density per chain, but total number of aldehydes per unit volume is similar between these samples (Fig. 1b). In fact, the unbinding force required to rupture adhesion between the probe and these two adhesives was statistically distinguishable ($p < 0.05$). Given that these experiments proceeded with the adhesives fully immersed and hydrated over hour timescales required of data acquisition, we considered that polymer degradation proceeded differently for

each sample and therefore the number of polymeric chains that interacted with available amine groups differed. To confirm this hypothesis, degradation kinetics of the different adhesive formulations was assessed (Fig. 1c). Indeed, 20% oxidation (composition D) results in significantly accelerated degradation rate compared with 50% oxidation (composition A). This finding is consistent with the hypothesis that composition D, having lower aldehyde groups density per chain, forms a network less efficiently and in turn that less densely crosslinked network will degrade more quickly upon immersion in aqueous solutions. In contrast, there was no statistically significant difference in degradation kinetics among samples A, B, and C. Thus, these data illustrate both a limitation of AFM-based screening of the loss of adhesive forces, and an advantage in that such rapid degradation and loss of adhesion capacity makes clear that such a composition is ill-suited to most *in vivo* adhesive sealant applications.

B. Macroscale failure load under normal loading

A facile and most commonly reported method of comparing tissue adhesives is uniaxial tensile loading of macroscale tissue-adhesive-tissue constructs, in which load is applied normal to the adhesive interface.[19,20] Interfacial strength of the tissue-adhesive specimens (Figs. 2a-b) was assessed by applying a constant displacement rate (0.05mm/s) normal to the tissue-adhesive-tissue interface (see Materials and Methods). As the interfacial area is difficult to quantify, failure is quantified by the maximum applied tensile load (rather than applied stress). Here we observed that the rupture of the tissue-adhesive-tissue structure occurred within the bulk of the adhesive for all tests, rather than at the tissue-adhesive interfaces. This finding demonstrates that these adhesives exhibited cohesive failure under this tensile mechanical loading mode. Although adhesive failure is the weakest link under this loading mode, the overall failure of the tissue-material-tissue construct is determined by both the material cohesive force and the adhesion strength at the tissue-material interface. If adhesive unbinding force is higher as a function of solid content, the tissue-material-tissue construct failure load would be expected to trend in the same manner even when the observed failure itself is cohesive. Hence, failure load for each composition (Fig 2c) was compared to the molecular-scale unbinding force (Fig. 1b). Indeed, a strong linear correlation (R^2=0.973) was observed. Thus, a concordance between molecular-scale F_R and macroscale failure load of the adhesive materials cured on excised rat small intestinal tissue exists.

However, we note that for the most anticipated applications of adhesives for small intestine repair, the adhesive will be applied atop an open wound on the tissue serosal layer and cured *in vivo*. The relevant loading state for such an application is better approximated by a measure of the burst pressure of the perfused organ. Next, we assessed interfacial strength through this macroscale method

C. Burst pressure under internal loading

Excised intestinal tissues comprising a hollow lumen were wounded and repaired with each adhesive polymer composition (see Materials and Methods). Following repair of a circular puncture wound, pulsatile loads were applied to the samples in a mechanical testing apparatus configured for luminal perfusion (Figs. 3a-b). Maximum luminal pressure prior to failure of the repair was recorded as burst pressure, indicating the adhesion strength under complex triaxial loading (Fig. 3c). Under these loading conditions, a correlation between this burst pressure and macroscopic failure load was found for compositions A, B, C. However, the PEG:dextran adhesive formulation with 20% oxidation (composition D, 10.4 ±0.53 kPa) demonstrated significantly higher burst pressure compared to 50% oxidation (composition A, 8.7±0.8 kPa , p = 0.032). Adhesive failure in the triaxial loading was at the tissue-material interface. For reference, physiological pressures of the duodenum are typically maximum at 4 kPa [21], indicating that all compositions failed at superphysiological perfusion pressures.

In contrast to the cohesive failure modes observed under uniaxial tensile loading, adhesive failure was observed under the burst pressure triaxial loading. In other words, failure of the seal always occurred directly at the tissue-material interface, as confirmed by the use of fluorescently labeled PEG in these PEG:dextran adhesives.[13]

D. *Ex vivo* adhesive interface morphology

To elucidate the difference between compositions A and D, samples with the same total number of aldehydes that differ in oxidation level and thus aldehyde density per chain, we examined the morphology of the interfacial region between these adhesives cured on top of, excised rat small intestinal tissues (Fig. 4). Quantitative fluorescence microscopy indicated significant differences in the adhesive regimes. Three distinct domains were observed: the bulk adhesive, the tissue, and the interfacial span between them. Clear differences were observed in terms of (1) the width of this interface; (2) the size and number of pores indicative of the extent of reaction with tissue amines; and (3) the existence of a visible gap between the fluorescently labeled adhesive material and the tissue itself. Composition A exhibited a wider interfacial region as well as higher pore area ($W=100.5\pm9.9$ μm and $\Phi=476.7\pm100.9$ μm^2) compared with composition D ($W=56.9\pm7.0$ μm and $\Phi=150.6\pm15.2$ μm^2). There was also a visible gap of fluorescence intensity along all tissue interfaces. In contrast, composition D exhibited smaller and fewer pores within a narrowed interfacial region, and no visible gap along a smoother interfacial line intersecting the tissue. This interface morphology demonstrates an improved interfacial adhesion and integration of the material. Quantification of fluorescence intensity at the interfacial regime corroborated this increased integration of fluorescently labeled adhesive at the interface (relative intensity of 14.1 ± 1.2 and 19.3 ± 2.3 for compositions A and D, respectively). However, given the rapid degradation of composition D upon extended immersion (Fig. 2b), composition D is a suboptimal adhesive for the *in vivo* application of small intestine sealing. For final optimization of adhesive materials *in vivo*, adhesion strength must be balanced with minimized inflammatory response. Next, we consider this issue for the two materials in this array that exhibit differential adhesion strength.

E. *In vivo* tissue interface pathology

The number of available aldehyde groups affects tissue biocompatibility, and can adversely offset the potential for strong tissue adhesion. [13] Here, we evaluated tissue response to compositions A and B, adhesives of significantly different resistance to uniaxial and multiaxial loading, without introducing high toxicity imparted by the significantly high solid content of composition C. The response to sutures alone was used as a control, and scoring of the immunohistological sections were compared (see Methods).

The overall inflammatory response did not extend beyond the area of healing, nor did it involve heterophilic infiltrates with necrosis. Composition A (8.75wt% dextran aldehyde) imparted negligible tissue response (score= 0), similar to that of suture alone (Fig. 5a). In contrast, composition B (14wt% dextran aldehyde) induced a higher inflammatory score (score= 2) including granoulomatous inflammation with lower re-epithelialization (Fig. 5b) and inflammatory infiltrates including histocytes and macrophages (Fig. 5c). These results reiterate the need to optimize adhesive materials in the context of both improved mechanical performance and tolerable *in vivo* response.

Discussion

It is increasingly appreciated that each tissue and application environment presents unique targets and demands on biomaterials, and thus the principles and approaches toward tissue-specific and application-specific materials design are of growing interest. For example, the pH, surface texture, tissue composition and structure of the liver, lung, gastrointestinal tract and

heart tissues are all significantly different. It is therefore plausible that similar materials will interact differently with each of these tissue types, as we have observed previously for PEG:dextran crosslinked hydrogels.[13] The present study demonstrates the ability to quantify the adhesion of a material to a target tissue by assaying for the pair components of the reaction sites on the tissue and material, requiring only small sample volumes compatible with higher throughput methods.

A. Effects of PEG:dextran polymer design at the molecular scale

As material aldehydes react with tissue amines, one can determine the potential binding force an aldehyde-based material would exhibit based on the number of free aldehyde groups and available tissue amines. Here, AFM probes were functionalized with amine groups to represent the tissue surface functionality. The unbinding force from the PEG:dextran adhesives was used to establish the binding or interaction potential of these adhesives to tissues exhibiting a range of amine-reactive groups. As would be required of such a small-scale materials optimization approach, the adhesive trends with composition observed via this molecular-scale method were correlated with those determined from macroscopic mechanical challenges under uniaxial and multiaxial *ex vivo* loading of the adhesive-tissue interface (section B).

B. Effect of material composition on failure resistance and modes

We found that increasing the solid content within PEG:dextran adhesive hydrogels was an efficient means to increase adhesion across all experimental length scales and loading challenges. Compositions A to C exhibited increased resistance to mechanical failure of the sealed interface, whether considering the nanoNewton-scale unbinding force of AFM force spectroscopy (Fig. 1), the Newton-scale failure force of tissue-adhesive-tissue constructs under normal loading (Fig. 2), or the Pa-scale burst pressures of sealed puncture wounds under triaxial loading (Fig. 3). The degree of crosslinking depends in part on the solid volume fraction within such hydrogels, as is consistent with the strong correlation between the molecular-scale unbinding force and the macroscale adhesive force under uniaxial loading of the interface for this series of compositions A through C (Fig. 2b).

We also varied %-dextran oxidation to alter the aldehyde density within the polymers of an otherwise comparable number of aldehyde groups (compositions A and D). We found that the resistance to macroscopic adhesive failure depended not only on the number of aldehydes per polymer chain within the hydrogel (A vs. D), but also on the loading form. This can be understood by the differences in extent of crosslinking between these formulations on one hand and the extent of reaction between dextran aldehydes and tissue amines at the other. While higher degree of oxidation results in more reactive groups per chain facilitating the interaction between aldehydes and amines and increases the extent of crosslinking, this is at the expense of tissue:material bond formation (Fig. 4). It is plausible that aldehydes in composition A form bonds with PEG amines more efficiently than with tissue amines, and thus resist better uniaxial failure where cohesive failure is observed. In contrast, aldehydes in composition D are distributed in a way that facilitates better reaction with tissue amines rather than PEG amines, thus resisting macroscopic failure under triaxial loading where failure is seen at the tissue:material interface. However, as noted above, the higher degradation rate of the more loosely crosslinked network of adhesive composition D decreased the utility of this material *in vivo*. When the objective of adhesive material optimization is to understand the most efficient means to increase failure strength, multiple means of mechanical characterization provide this capacity. Here, by comparing the failure modes (adhesive vs. cohesive) and effects of compositions (number vs. density of aldehyde groups) among three mechanical characterization approaches, we inferred the extent to which dextran aldehydes react with PEG amines (within the adhesive material) vs. tissue amines (at the tissue-adhesive interface).

C. Further consideration of application-relevant measurements of 'adhesion strength'

The resistance to adhesive failure, if measured as the stress (or even load) required to disrupt the integrity of the material interface is often loosely termed 'adhesion strength'. More accurately, this quantity is a loss of adhesion between two surfaces, and can arise as a result of loss of the interfacial strength conferred by adhesion or intramaterial interactions determined by cohesion. The adhesion strength of materials to biological tissues is commonly characterized by tensile or peel tests.[22,23] Measurement of adhesion of specific chemical groups to specific surfaces is an emerging approach [24,25] that can provide additional insight. Lee et al. reported adhesion strength of single DOPA residue to a wet metal oxide surface via AFM force spectroscopy [11], quantified by estimating the magnitude of bond dissociation energy. While previous measures of material-tissue interaction focused on the potential chemical interactions at the multimolecular scale or the resistance to adhesive failure at the macroscale, we now compare these two lengthscales and measures of adhesive material performance directly. Additionally, we have noted that the predictive capacity of macroscopic ex vivo experiments requires that this mechanical loading is designed in context of *in vivo* application loading and state.

Although there are several distinct types of macroscale mechanical tests to quantify the resistance to adhesive failure between surfaces, the stress states exerted on the material and the interface during tensile tests, peel tests or burst pressure tests are different. As a result, even the trends in failure resistance with adhesive material composition can depend on mechanical loading. For example, Ono et al. demonstrated that inverse trends can result when testing materials in tensile or burst modes.[26]

AFM-enabled force spectroscopy and macroscale tissue-adhesive-tissue rupture experiments approximate a uniaxial tensile stress state at the interface, and hence these failure loads were well correlated (Figs. 1b vs. 2c). In contrast, the tissue samples in the burst pressure experiment are under a more complex, multiaxial stress state (Fig. 3b). With this in mind, it is not surprising that composition D, despite displaying decreased cohesive strength compared to composition A (Fig. 2c), presented a higher macroscopic burst pressure under the triaxial stress state most representative of perfused organs such as the small intestine (Fig. 3c). Our experiments demonstrate that the distribution of aldehyde groups along the exposed chains plays a key role in adhesion to these tissues for the practical application of interest: sealing of open serosal wounds of the small intestine subjected to perfusion pressure. Thus, adhesive materials for *in vivo* use requires that macroscale experiments would reflect the mechanical loading states anticipated for wound sealing applications *in vivo*.

D. Targeting adhesive polymers for specific tissues and applications

Our *in vivo* studies revealed increasing cytotoxicity of the PEG:dextran hydrogels with increasing solid content. Both the adhesion score and inflammatory response were higher in composition B than in composition A. In fact, composition A, presented a tissue response comparable to that of suture alone, demonstrating that lowering the adhesive aldehyde content reduces the adverse biocompatibility effect of the sealant. Although molecular-scale and macroscale measures of adhesion failure resistance can facilitate design of new adhesive polymer families, biocompatibility remains an important component of adhesive material optimization. Even in these adhesives comprising biocompatible constituents, higher adhesion and failure strength *ex vivo* can correlate with increasingly adverse tissue reactions *in vivo*. The requirements on materials rise as applications increase in complexity. Adhesive sealing of duodenal wounds for example, requires, a composition exhibiting high burst pressure (to prevent leakage of gut content after internal surgery), low degradation rate, and minimal inflammatory response. The family of PEG-dextrans we are considering demonstrates that: (1) increased aldehyde content correlates with adhesion strength for all modes of evaluation, but

also an increased inflammatory response; (2) lower aldehyde density correlates with increased burst pressure failure and improved interfacial morphology of the serosal wound, but also increased degradation rates *in vivo*; and (3) all adhesive materials considered exhibited superphysiologic interfacial failure strengths under the anticipated in vivo mechanical loading challenge. Thus, for the specific applications of interest in vivo: sealing of open serosal wounds of the small intestine, composition A which is comprised of 10kDa dextran aldehyde with 50% oxidation and 8.75wt% (D10-50-8.75 P8-10-25) provides an optimal balance of mechanical performance, seal stability over time and biological tolerance.

Conclusions

Polymer materials designed as adhesives for biological applications require optimization of interfacial failure resistance, degradation rates, and biocompatibility. When the interfacial chemical reactions between the adhesive and tissue target are well defined, such as in the case of PEG:dextran adhesives and soft-tissue organs such as the duodenum, mechanical characterization of this adhesion potential can be quantified across lengthscales and mechanical conditions. AFM-enabled force spectroscopy offers the opportunity to define a specific binding potential for a given material and a given target tissue, and is predictive of the macroscale resistance to adhesive failure modes for the adhesive sealants and tissues considered herein. Ultimately, the macroscopic characterization of failure should consider mechanical loading profiles relevant to the tissue/organ application of interest. Finally, while this resistance to failure of an adhesively sealed tissue interface is an important factor in development of materials for biological sealants, *in vivo* experiments are still required to optimize the ‘adhesion strength’ in the context of sufficient biocompatibility.

Supplementary Material

Refer to Web version on PubMed Central for supplementary material.

Acknowledgments

The authors acknowledge KJVV: NSF CAREER Award; ASZ: NDSEG Fellowship and ERE National Institutes of Health (GM 49039).

References

[1]. Hilgert LA, Lopes GC, Araujo E, Baratieri LN. Adhesive procedures in daily practice: essential aspects. Compend Contin Educ Dent May;2008 29(4):208–15. quiz 16, 18. [PubMed: 18524205]

[2]. Berdahl JP, Johnson CS, Proia AD, Grinstaff MW, Kim T. Comparison of sutures and dendritic polymer adhesives for corneal laceration repair in an in vivo chicken model. Archives of ophthalmology Apr;2009 127(4):442–7. [PubMed: 19365021]

[3]. Saunders MM, Baxter ZC, Abou-Elella A, Kunselman AR, Trussell JC. BioGlue and Dermabond save time, leak less, and are not mechanically inferior to two-layer and modified one-layer vasovasostomy. Fertility and sterility Feb;2009 91(2):560–5. [PubMed: 18304547]

[4]. Martens TP, Godier AF, Parks JJ, Wan LQ, Koeckert MS, Eng GM, et al. Percutaneous cell delivery into the heart using hydrogels polymerizing in situ. Cell transplantation 2009;18(3):297–304. [PubMed: 19558778]

[5]. Papatheofanis FJ, Ray RD. Experimental use of adhesives in the repair of transverse fractures of the rat and rabbit. Biomaterials, medical devices, and artificial organs 1983;10(4):247–65.

[6]. Tireli E, Ugurlucan M. eComment: Fibrin glue reinforced Teflon felt sandwich for the prevention of anastomotic leak in replacement of ascending aorta for acute aortic dissection. Interactive cardiovascular and thoracic surgery Aug;2009 9(2):212–3. [PubMed: 19628539]

[7]. Hall RC, Logan AJ, Wells AP. Comparison of fibrin glue with sutures for pterygium excision surgery with conjunctival autografts. Clinical & experimental ophthalmology Aug;2009 37(6):584–9. [PubMed: 19702708]

[8]. Maniwa T, Kaneda H, Saito Y. Management of a complicated pulmonary fistula caused by lung cancer using a fibrin glue-soaked polyglycolic acid sheet covered with an intercostal muscle flap. Interactive cardiovascular and thoracic surgery Jun;2009 8(6):697–8. [PubMed: 19270019]

[9]. Vinatier C, Gauthier O, Masson M, Malard O, Moreau A, Fellah BH, et al. Nasal chondrocytes and fibrin sealant for cartilage tissue engineering. Journal of biomedical materials research Apr;2009 89(1):176–85. [PubMed: 18431767]

[10]. Lee H, Lee BP, Messersmith PB. A reversible wet/dry adhesive inspired by mussels and geckos. Nature Jul 19;2007 448(7151):338–41. [PubMed: 17637666]

[11]. Lee H, Scherer NF, Messersmith PB. Single-molecule mechanics of mussel adhesion. Proceedings of the National Academy of Sciences of the United States of America Aug 29;2006 103(35):12999–3003. [PubMed: 16920796]

[12]. Mahdavi A, Ferreira L, Sundback C, Nichol JW, Chan EP, Carter DJ, et al. A biodegradable and biocompatible gecko-inspired tissue adhesive. Proceedings of the National Academy of Sciences of the United States of America Feb 19;2008 105(7):2307–12. [PubMed: 18287082]

[13]. Artzi N, Shazly T, Baker AB, Bon A, Edelman ER. Aldehyde-Amine Chemistry Enables Modulated Biosealants with Tissue-Specific Adhesion. Adv Mat 2009;21(32):3399–403.

[14]. Shazly TM, Artzi N, Boehning F, Edelman ER. Viscoelastic adhesive mechanics of aldehyde-mediated soft tissue sealants. Biomaterials Dec;2008 29(35):4584–91. [PubMed: 18804861]

[15]. Artzi N, Shazly T, Crespo C, Ramos AB, Chenault HK, Edelman ER. Characterization of star adhesive sealants based on PEG/dextran hydrogels. Macromolecular bioscience Aug 11;2009 9(8): 754–65. [PubMed: 19384975]

[16]. Cleveland JP, Manne S, Bocek D, Hansma PK. A nondestructive method for determining the spring constant of cantilevers for scanning force microscopy. Review of Scientific Instruments 1993;64 (2):403–5.

[17]. Lee S, Mandic J, Van Vliet KJ. Chemomechanical mapping of ligand-receptor binding kinetics on cells. Proceedings of the National Academy of Sciences of the United States of America Jun 5;2007 104(23):9609–14. [PubMed: 17535923]

[18]. Van Vliet KJ, Bao G, Suresh S. The biomechanics toolbox: Experimental approaches for living cells and biomolecules. Acta Materialia 2003;51:5881–905.

[19]. Azadani AN, Matthews PB, Ge L, Shen Y, Jhun CS, Guy TS, et al. Mechanical properties of surgical glues used in aortic root replacement. The Annals of thoracic surgery Apr;2009 87(4):1154–60. [PubMed: 19324142]

[20]. Rickett T, Li J, Patel M, Sun W, Leung G, Shi R. Ethyl-cyanoacrylate is acutely nontoxic and provides sufficient bond strength for anastomosis of peripheral nerves. Journal of biomedical materials research Sep 1;2009 90(3):750–4. [PubMed: 18570316]

[21]. Kalloo AN, Pasricha PJ. Effect of gastric distension and duodenal fat infusion on biliary sphincter of Oddi motility in healthy volunteers. Digestive diseases and sciences Apr;1995 40(4):745–8. [PubMed: 7720464]

[22]. Nussinovitch A, Gal A, Padula C, Santi P. Physical characterization of a new skin bioadhesive film. AAPS PharmSciTech 2008;9(2):458–63. [PubMed: 18431662]

[23]. Wilson DJ, Chenery DH, Bowring HK, Wilson K, Turner R, Maughan J, et al. Physical and biological properties of a novel siloxane adhesive for soft tissue applications. Journal of biomaterials science 2005;16(4):449–72.

[24]. Pirzer T, Geisler M, Scheibel T, Hugel T. Single molecule force measurements delineate salt, pH and surface effects on biopolymer adhesion. Physical biology 2009;6(2):025004. [PubMed: 19571365]

[25]. Sonnenberg L, Parvole J, Kuhner F, Billon L, Gaub HE. Choose sides: differential polymer adhesion. Langmuir Jun 5;2007 23(12):6660–6. [PubMed: 17489614]

[26]. Ono K, Saito Y, Yura H, Ishikawa K, Kurita A, Akaike T, et al. Photocrosslinkable chitosan as a biological adhesive. J Biomed Mater Res Feb;2000 49(2):289–95. [PubMed: 10571917]

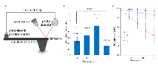

Figure 1.
(a) Schematic of AFM cantilevered probes functionalized with amine groups used to measure the rupture force between free amines and adhesive formulations, (b) rupture force for variation in the relative number of free aldehyde groups (compositions A-C; D10-50-8.75, D10-50-14, D10-50-18 with P8-10-25) or aldehyde group density (composition D; D10-20-23 P8-10-25), (c) degradation kinetics of different adhesive formulations listed above. Values reported as average ± standard error.

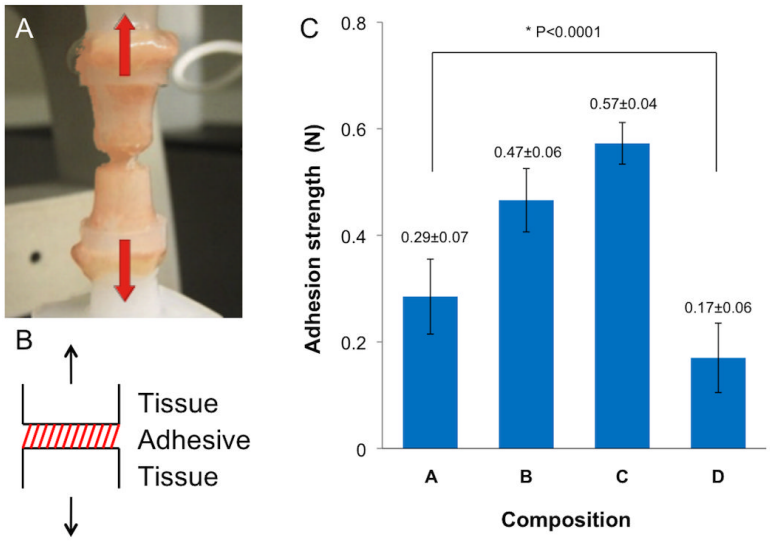

Figure 2.

(a) Image and (b) schematic of tissue-material-tissue interface in uniaxial tensile loading, (c) adhesion strength of compositions A-D applied to a rat small intestine. Values reported as average ± standard deviation.

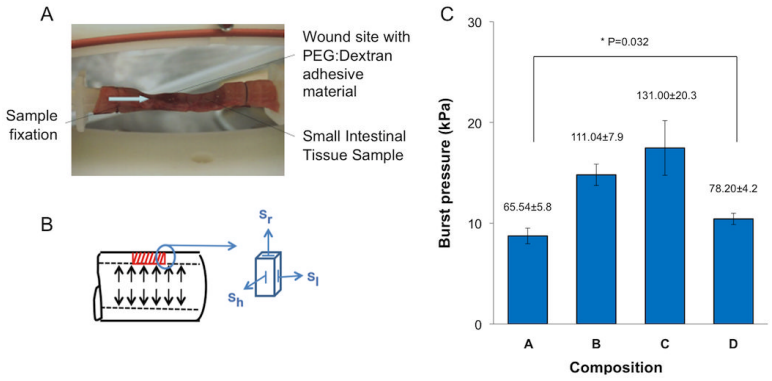

Figure 3.

(a) Image and (b) schematic of burst pressure experiment; stresses within and at the interface are multiaxial, including interfacial shear as well as radial, longitudinal and hoop stresses σ_r, $\sigma_l$and σ_h,(c) burst pressure of compositions A-D applied to a rat small intestine. Values reported as average ± standard deviation.

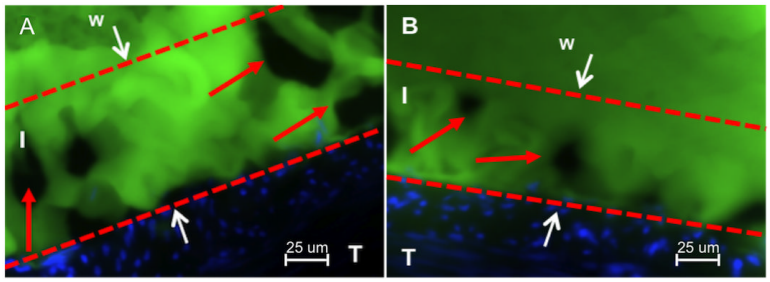

Figure 4.

Morphology of the interfacial region between the two material formulations and excised rat small intestinal tissues using quantitative fluorescence microscopy. (a) composition A with 50% oxidation, D10-50-8.75 P8-10-25 (relative intensity 19.3±2.3) (b) composition D with 20% oxidation, D10-20-23 P8-10-25 (relative intensity 14.1±1.2). Three distinct regions are shown, T- tissue, I-interfacial region between the tissue and the adhesive material and B-bulk adhesive material.

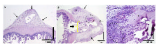

Figure 5.
Hematoxylin and Eosin staining of rabbit small intestinal tissue after 15 days of adhesive application with (a) composition A; D10-50-8.75 P8-10-25 (b) composition B; D10-50-14 P8-10-25. Scale bar is 1 mm. (c) magnification of the dashed area seen in figure 5b. scale bar is 200μm.

Table 1

Compositional description of the examined PEG:dextran compositions

Composition	Name	Dextran aldehyde			PEG amine			PEG:Dextran
		Molecular weight (kDa)	Percent oxidation (%)	Solid content (%)	Arm number (#)	Molecular weight (kDa)	Solid content (%)	Reactive group ratio (CHO:NH_2)
D10-50-8.75 P8-10-25	A	10	50	8.75	8	10	25	3
D10-50-14 P8-10-40	B	10	50	14	8	10	40	3
D10-50-18 P8-10-50	C	10	50	18	8	10	50	3
D10-20-23 P8-10-25	D	10	20	23	8	10	25	3